

Steel waste as an adsorbent for removing sodium naphthalene sulfonate from aqueous media

José Adson Pereira dos Santos^a, Ronaldo Ferreira do Nascimento^a

^a Department of Analytical Chemistry and Physical-Chemistry, Federal University of Ceara, 60455-970, Fortaleza, Ceara, Brazil.

Abstract

Sodium naphthalene sulfonate (SNS), a toxic contaminant found in many industrial effluents, was removed from an aqueous solution using a low-cost material derived from steel industry waste, blast furnace sludge (BFS). FTIR analysis was employed to characterize the adsorbent before and after the adsorption process, providing information on the composition, structure, and interaction between SNS and BFS. Pseudo-first and pseudo-second-order reaction kinetics models, as well as the Weber-Morris intraparticle diffusion model and the Mathews-Weber external diffusion model, were used to investigate the adsorption kinetics. The Origin software was used to apply the kinetic models in a non-linear form to the experimental data, providing the statistical parameters of the fit. The kinetic models provided crucial information on the limiting steps of the process, as well as values for the rate constant and equilibrium capacity. The contaminant was efficiently adsorbed by BFS, achieving over 60% removal in less than 10 minutes.

Keywords: Blast furnace sludge (BSF); Sodium naphthalene sulfonate (SNS); Adsorption kinetic

1. Introduction

For every ton of steel processed, approximately 2 to 3 tons of waste is generated as solid byproducts [1]. These wastes are predominantly composed of dust and slag. The dust undergoes a gas-washing process, forming sludge, a particulate material primarily composed of iron oxides, zinc oxide, carbon, and alkalis [2]. Measures such as waste reutilization contribute to developing environmentally responsible processes by establishing more sustainable industrial methods. In the case of steelmaking waste, there are various possibilities for its reuse, including its use as low-cost adsorbents for the remediation of environmental contaminants, such as toxic metals and refractory organic compounds (textile dyes and industrial additives) [3]. Currently, a variety of steelmaking wastes have been widely applied in adsorption processes aimed at removing inorganic and organic pollutants from aqueous matrices and industrial effluents.

In this context, sodium naphthalene sulfonate (SNS), a universal dispersant widely used in the textile, tanning, construction, and oil well drilling industries, among other industrial activities [4], plays a significant role as a contaminant in effluents. It is found in various industrial effluents and is

considered a refractory organic compound harmful to human health and the environment [5]. This study investigated the kinetic behavior of sodium naphthalene sulfonate (SNS) adsorption in synthetic effluent, considering the pH and conductivity conditions of a textile effluent. Blast furnace sludge (BFS), a low-cost steelmaking waste produced in large quantities, was used as the adsorbent. In addition to the application of kinetic models, Fourier transform infrared spectroscopy (FTIR) analysis was employed to obtain information on the interaction between SNS and BFS.

2. Materials and methods

2.1 Reagents and Materials

The commercial sodium naphthalene sulfonate was purchased from Auros Química (Brazil) and used without any purification process. The sodium chloride and sodium hydroxide, both reagent grade, were obtained from Dinâmica (Brazil).

The adsorbent material used was blast furnace slag (BFS) provided by Companhia Siderúrgica do Pecém (Brazil). The material was used after drying and grinding. Drying was carried out in an oven at 105 °C until constant mass was achieved. Grinding

was done using a mortar and pestle, resulting in a uniform and finely divided powder.

2.2 Characterization of the adsorbent material before and after adsorption

BFS samples were characterized before and after adsorption by Fourier transform infrared spectroscopy (FTIR) using a Shimadzu IRTracer 100 spectrophotometer, in the range of 400 to 4000 cm^{-1} . The samples were prepared as pellets with KBr powder.

2.3 Adsorption of sodium naphthalene sulphonate by BFS

2.3.1 Aqueous synthetic effluent

The synthetic effluent was prepared by dissolving 0.0270 g of SNS in 1 L of distilled water. To adjust the pH and conductivity conditions to values close to those of a textile effluent, the conductivity of the solution was adjusted to 8 mS/cm using 2.0 mol L^{-1} NaCl, and the pH was adjusted to 10 with 0.1 mol L^{-1} NaOH.

2.3.2 Adsorption kinetics

The kinetic experiments were performed in triplicate, using 0.05 g of the adsorbent and 25 mL of a solution containing SNS (27 mg L^{-1}). The mixtures were agitated at 200 rpm on an orbital shaker at a temperature of 28 ± 2 °C. After adsorption, with contact times ranging from 0 to 180 minutes, the mixtures were centrifuged of at 5000 rpm, and the concentration of SNS in the supernatant was determined by UV-Vis spectrophotometry using a Shimadzu spectrophotometer, model UV-1800. Measurements were taken using a quartz cuvette with a 1 cm optical path and a wavelength of 227 nm.

The software Origin, version 2019b, was employed to apply the kinetic models in non-linear form to the experimental data, providing the model parameters and the statistical values of the fit.

3. Results and discussion

3.1 Characterization of BFS before and after adsorption test

The adsorption sites (oxides) of the material were investigated by FTIR. The FTIR spectrum obtained for BFS is shown in Fig. 1(a). The spectrum presents two bands at 1414 and 869 cm^{-1} , corresponding to the C-O bond stretching and CO_3^{2-} bending vibrations from calcite [6]. BFS also exhibits a strong intensity band at 998 cm^{-1} , related to the O-H bond vibrations of iron oxyhydroxides and the O-S-O bond vibrations from silica and silicates [7]. The bands between 535 and 453 cm^{-1} are associated with the Fe-O bond vibrations of iron oxides [8].

Fig. 1(b) presents the FTIR spectrum for SNS, characterized by strong intensity bands at 1179, 1116, and 1034 cm^{-1} , which are related to the symmetric and asymmetric stretching vibrations of the $-\text{SO}_3^-$ bonds, respectively [9]. The bands at 895 and 830 cm^{-1} are attributed to the substituted ring structure [10].

Fig. 1(c) shows the spectrum of the adsorbent after the adsorption process, where it is observed that the adsorbent material maintained its identity, indicating stability during the adsorption process. The spectrum also shows the appearance of a band at 1099 cm^{-1} , related to the adsorption of SNS on BFS. This band represents the $-\text{SO}_3^-$ bond vibrations, which, upon interacting with BFS, experience a shift, indicating a chemical interaction between SNS and the adsorbent [11].

3.2 Adsorption kinetics

Fig. 2(a) shows the percentage removal of SNS as a function of contact time with BFS. It is observed that removal reaches equilibrium at approximately 60 minutes, achieving 70% removal. In Fig. 2(b), the pseudo-first-order (PFO) [12], pseudo-second-order (PSO) [13], Weber-Morris [14], and Mathews-Weber [15] models applied to the experimental data are presented. The model parameters and errors (sum of squared errors, SSE) are described in Table 1. The PSO model provided the best fit, with a determination coefficient ($R^2 = 0,9994$) and error ($\text{SSE} = 0,0387$). The high correlation of the experimental data with the PSO model may indicate an abundance of active sites in

BFS, suggesting a chemical adsorption mechanism, as evidenced by the FTIR characterization [16].

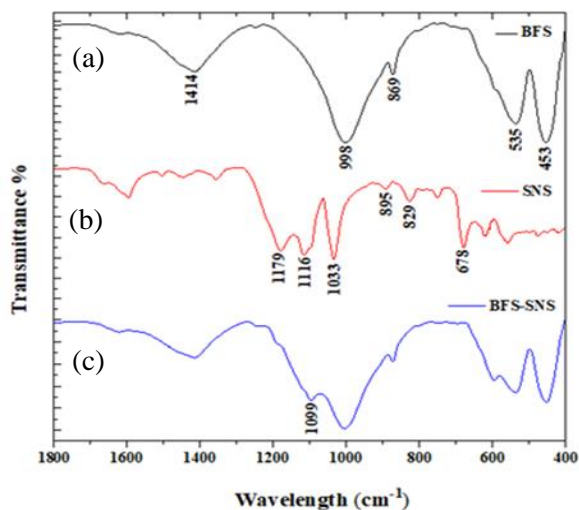


Fig. 1. FTIR spectra (a) of the BFS adsorbent, (b) FTIR of the SNS and (c) of the adsorbent after adsorption.

The equilibrium adsorption capacity, calculated based on the PSO model, was $10.4686 \text{ mg}\cdot\text{g}^{-1}$, while the initial adsorption rate, given by $h = k_2q_e^2$, was

$8.1974 \text{ mg}\cdot\text{min}^{-1}\cdot\text{g}^{-1}$. The high removal rate in the first minutes of the process may be related to the presence of active sites on the surface of the BFS, as well as the presence of mesopores in the adsorbent [17].

The models based on Weber-Morris intraparticle diffusion and Mathews-Weber external diffusion were used to better elucidate the adsorption mechanism. For the application of the Weber-Morris intraparticle diffusion model, the experimental data were divided into two segments: the first from 0 to 2 minutes, and the second from 4 to 10 minutes. Considering the value of the determination coefficient ($R^2 = 0.9954$), the Weber-Morris model was the best fit to the experimental data, indicating that the intraparticle diffusion process is one of the rate-limiting steps in this adsorption process [18].

The rate constant k_{WM1} indicates that the adsorption rate is fast in the first stage, while in the second stage, characterized by the rate constant k_{WM2} , the adsorption rate is slower. This is likely due to the initial filling of the pores, resulting in a momentary equilibrium and requiring the adsorbate to migrate to the regions of active sites, allowing more adsorbate molecules to diffuse through the pores [14].

Table 1. Results of applying kinetic models to SNS adsorption.

Model	R ²	SSE	Parameters
PFO	0,9943	0,3528	$q_e = 9,0878 \text{ mg}\cdot\text{g}^{-1}$ $k_1 = 0,5737 \text{ min}^{-1}$
PSO	0,9994	0,0387	$q_e = 10,4686 \text{ mg}\cdot\text{g}^{-1}$ $k_2 = 0,0748 \text{ g}\cdot\text{mg}^{-1}\cdot\text{min}^{-1}$
Weber-Morris	0,9956	0,2704	$k_{WM1} = 4,7763 \text{ mg}\cdot\text{g}^{-1}\cdot\text{min}^{1/2}$ $k_{WM2} = 0,3355 \text{ mg}\cdot\text{g}^{-1}\cdot\text{min}^{1/2}$
Mathews-Weber	0,7994	12,4606	$k_c = 6,5753 \text{ cm}\cdot\text{min}^{-1}$ $S = 0,0251 \text{ cm}^{-1}$

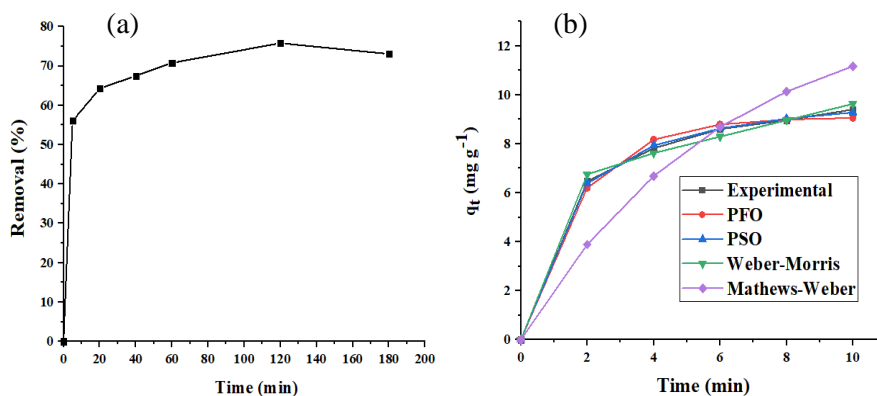


Fig. 2 (a) SNS removal by contact time with the BFS and (b) non-linear fit of the pseudo-first-order, pseudo-second-order, Weber-Morris and Mathews-Weber kinetic models, in the interval 0 - 10 minutes.

4. Conclusion

The blast furnace sludge used as an adsorbent in this study efficiently removed sodium naphthalene sulfonate from the aqueous solution, proving to be a promising adsorbent for the removal of this contaminant. The equilibrium adsorption capacity, estimated by the pseudo-second-order model, was $10.4686 \text{ mg} \cdot \text{g}^{-1}$, with over 60% of the SNS being removed within the first 10 minutes. The application of kinetic models, together with FTIR characterization, shows that the rate-limiting steps of the process are related to adsorption at active sites and intraparticle diffusion, with the models showing determination coefficients higher than 0.99.

Acknowledgements

The authors thank the Analytical Center of the Graduate Program in Chemistry at the Federal University of Ceará, as well as the Vibrational Spectroscopy and Microscopy Laboratory (LEVM) of the Department of Physics at UFC for the FTIR analyses.

References

- [1] Szekely J. Steelmaking and Industrial Ecology. Is Steel a Green Material?. *ISIJ International*, v.36 n.1, p.121-132, 1996.
- [2] Ashrit S, Chatti R, Sarkar S. Identification of the carbon source in blast furnace flue dust through characterization and statistical analysis. *International Journal of Environmental Analytical Chemistry*, v.101 n.10, p.1378-1392, 2021.
- [3] Ghosh, A., Ghosh, A. K. *Solid Waste Management in Steel Industry—Challenges and Opportunities. In Sustainable Waste Management: Policies and Case Studies* (pp. 299–307), 2020. Springer Singapore.
- [4] Karthikeyan S, Jo W, Dhanalakshmi R et al. A porous activated carbon supported Pt catalyst for the oxidative degradation of poly[(naphthaleneformaldehyde)sulfonate]. *Journal of the Taiwan Institute of Chemical Engineers*, 289-297, 93, 2018.
- [5] Wolf C, Storm T, Lange F et al. Analysis of Sulfonated Naphthalene–Formaldehyde Condensates by Ion-Pair Chromatography and Their Quantitative Determination from Aqueous Environmental Samples. *Analytical Chemistry*, 5466-5472, 72(21), 2000.
- [6] Bessler K, Rodrigues L. Os polimorfos de carbonato de cálcio: uma síntese fácil de aragonita. *Química Nova*, 178-280, 31(1), 2008.
- [7] Navarro, C, Díaz, M, Villa-García, M. A. Physico-Chemical Characterization of Steel Slag. Study of its Behavior under Simulated Environmental Conditions. *Environmental Science & Technology*, v. 44, n. 14, p. 5383–5388, 15 jul. 2010.
- [8] Wladimirsky A, Palacios D, Coggiola E et al. Spectroscopic investigations of iron(II) and iron(III) oxalates. *J. Braz. Chem. Soc.*, 20, p.445-450, 2009.
- [9] Xu F, Cai Y, Qian W et al. Characterization and mechanism analysis of polynaphthalene sulfonate modified cemented soil. *Construction and Building Materials*, 117936, 240, 2020.
- [10] Fekry M, Shafek S, Soliman F et al. Impact of poly naphthalene sulfonate on the dispersion stability of iron oxide nanoparticles. *Egyptian Journal of Petroleum*, 23-32, 32(1), 2023.
- [11] Yang B, Guan Z. Upgrading silicon-calcareous phosphate ores using sodium polymer [(Naphthalene formaldehyde) sulfonate] (PNFS) as an efficient and eco-friendly depressant. *Minerals Engineering*, 108075, 197, 2023.
- [12] Lagergren, S. About the theory of so-called adsorption of soluble substances. *K.Sven. Vetenskapsakad. Handl.* 24, 1–39, 1898.
- [13] Y.S. Ho, D.A.J. Wase, C.F. Forster Removal of lead ions from aqueous solution using sphagnum moss peat as adsorbent *Water. SA*, 22, pp. 219-224, 1996.
- [14] J. Wang, X. Guo. Repensando o modelo de cinética de adsorção por difusão intrapartícula: interpretação, métodos de resolução e aplicações. *Chemosphere*, 309, Artigo 136732, 2022.
- [15] Mathews, A.R., Weber, A.W.J. Modeling and parameter evaluation for adsorption in slurry reactors. *Chem. Eng. Commun.* 25, 157–17, 1984.
- [16] Wang, J., Guo, X. Adsorption kinetic models: physical meanings, applications, and solving methods. *J. Hazard Mater.* 390, 122156, 2020.
- [17] Da Silva J, Da Silva C, Freire J et al. Industrial steel waste-based adsorbent: An effective phosphate removal from aqueous media. *Materiais Chemistry and Physics*, 126828, 292, 2022.
- [18] Wang Y, Wang C, Huang X et al. Guideline for modeling solid-liquid adsorption: Kinetics, isotherm, fixed bed, and thermodynamics. *Chemosphere*, 140736, 349, 2024.